Available online at www.sciencedirect.com
SCIENCE DIRECT®
ELSEVIER
Nuclear Instruments and Methods in Physics Research B 219–220 (2004) 405–409
NIM B
Beam Interactions with Materials & Atoms
www.elsevier.com/locate/nimb

# The new Surrey ion beam analysis facility

A. Simon [a,1], C. Jeynes [a,*], R.P. Webb [a], R. Finnis [a], Z. Tabatabaian [a], P.J. Sellin [b], M.B.H. Breese [c], D.F. Fellows [d], R. van den Broek [e], R.M. Gwilliam [a]

[a] *The Nodus Laboratory, University of Surrey Ion Beam Centre, Guildford, Surrey GU2 7XH, UK*
[b] *Department of Physics, University of Surrey, Guildford GU2 7XH, UK*
[c] *Department of Physics, National University of Singapore, Singapore 119 228*
[d] *Arun Microelectronics Ltd., Fitzalan Road, Arundel BN18 9JP, West Sussex, UK*
[e] *High Voltage Engineering B.V., 3800 AB Amersfoort, The Netherlands*

**Abstract**

We present the characteristics of an ion beam analysis facility based on a fully computer controlled 2 MV Tandetron™ commissioned in 2002. The terminal voltage temperature stability is measured using the 3036 keV $^{16}O(\alpha,\alpha)^{16}O$ resonance. A microbeam beamline with an Oxford triplet lens and a coolable sample holder has been built. We report new temperature dependent time-resolved IBIC measurements from CZT detectors that illustrate the capability of the system. A millibeam beamline has been built with a 6-axis goniometer capable of handling 100 mm wafers through an airlock with a *z*-axis for the precise location of the sample surface at the eucentric point. This instrument is designed for routine RBS/ERD and channelling applications, and incorporates a versatile controller capable of fully automated data collection.


## 1. The accelerator

A new 2 MV Tandetron™ [1] accelerator from High Voltage Engineering Europe capable of unattended overnight running was installed at the University of Surrey and commissioned in Spring 2002. The anti-ripple instrumentation described by Mous et al. [2] is fitted giving a voltage stability expected to be better than 50 V. A 90° low energy magnet accommodates two ion sources and a 5-port high energy magnet has two 10° and two 30° ports. A millibeam is fitted to a 10° port and a microbeam to a 30° port.

The accelerator provides an extremely stable beam, with beam current on target varying by less than 1% over 5 minutes and drifting by less than 5% over several hours. Energy stabilisation using feedback from either the low energy or the high energy magnet slits is not required to achieve this. However, the system is sensitive to the calibration of the generating voltmeter (GVM) which provides the system energy reference and depends on dimensional stability. We have observed thermal drift in this instrument by monitoring the backscattering

* Corresponding author. Tel.: +44-1483-686096/689829; fax: +44-1483-689404/689391.
*E-mail address:* c.jeynes@surrey.ac.uk (C. Jeynes).
[1] On leave from: Institute of Nuclear Research, Hungarian Academy of Sciences (ATOMKI), Debrecen, Hungary.

0168-583X/$ - see front matter © 2004 Elsevier B.V. All rights reserved.
doi:10.1016/j.nimb.2004.01.091

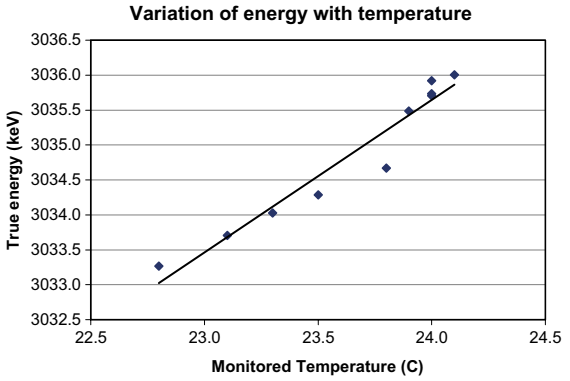


Fig. 1. Temperature coefficient of Tandetron terminal voltage using a $^4He^+$ beam.

yield of the 3036 keV $^{16}O(\alpha,\alpha)^{16}O$ resonance (Fig. 1). At the resonance energy the yield is very sensitive to the precise energy of the beam. Fig. 1 shows that the temperature coefficient of the terminal high voltage due to the thermal drift in the GVM is about 1 kV/°C or about 0.07%/°C.

## 2. Microprobe beam line

The focussing system is an quadrupole triplet [3] from Oxford Microbeams Ltd. The object distance is 6.3 m while the image distance is 16 cm, giving demagnifications of $D_x = 74$ in the horizontal plane and $D_y = 22$ in the vertical one, as calculated using the PRAM computer code [4]. Typically 2 μm sized proton beams have been reached easily and routinely. Improved object slits will shortly allow 1 μm resolution.

Two sets of manual micrometer driven slits are installed: the object aperture close to the magnet and the divergence limiting aperture immediately before the scanning coils. To reduce vibration, both of the object aperture and lens (including the beam divergence aperture, the scanning coils and the target chamber) assemblies are mounted on concrete blocks, and are separated from the high energy magnet and the long flight tube with bellows, as is the (magnetic levitation) turbopump for the target chamber.

The beam brightness of the accelerator is typically $B = 1$ pA/(μm$^2$ mrad$^2$ MeV) for 2 MeV $H^+$ and $B = 0.5$ pA/(μm$^2$ mrad$^2$ MeV) for 2 MeV $He^{2+}$ at a divergence of 0.08 mrad. These values are comparable to other reports of duoplasmatron sources (see in [5]). Note that these values are indicative: we have observed a much higher value of 8 pA/(μm$^2$ mrad$^2$ MeV) for 2 MeV $H^+$.

The octagonal target chamber from Oxford Microbeams Ltd. is designed for a small image distance (18 cm from the end of the lens to the target) and hence a high demagnification. A 3-axes Huntington PM-600 TRC Precision XYZ sample stage with 2 microns movement precision is mounted onto the lid. An 80 mm$^2$ Si(Li) detector with a 12.5 μm thick Be window is installed at a backward angle of 45° for PIXE spectroscopy at a distance from the sample of between 25 and 70 mm. A particle detector is also mounted above the entrance of the beam ($\Theta = 165°$, $\Omega = 16.5$ msr), where the fluence incident on the sample is determined from simultaneously collected RBS spectra (using the "$Q$-factor" method [6]). In transmission geometry a Hamamatsu S1223 Si photodiode and a carbon Faraday cup are mounted onto a rotating flange, making available measurements of both beam current and the on-axis and off-axis transmission. Data is collected on an event by event basis (listmode) with the data acquisition (OM-DAQ) system from Oxford Microbeams Ltd. Beam current can also be monitored directly from the isolated sample stage.

The microbeam chamber is fitted with a sample stage temperature controlled over the range 80–300 K and a temperature stability of better than ±5 K. The sample plate is attached to a heater block on a LN-cooled cold-finger. A 1.3 l liquid nitrogen dewar requires refilling every 2 h. The sample plate is mechanically connected to the chamber lid via a plastic rod to minimise thermal displacement and vibration of the sample during cooling, which is typically 100 μm vertical displacement of the sample when cooling from 300 K to 100 K.

The excellent spatial resolution and stability of the microbeam provides a powerful tool for ion beam induced charge (IBIC) imaging of bulk semiconductor (including II–VI, III–V and group IV) materials. Conventional IBIC imaging [4] of pulse amplitude in these materials provides quan-

titative high resolution maps of charge collection efficiency (CCE) and charge carrier drift lengths. These data give insight into the distribution and nature of charge traps in bulk semiconductor materials. IBIC imaging of charge transport inside individual crystallites of CVD diamond has been used to measure intra-crystallite CCE and to show the concentration of trapping centres at the crystallite boundaries [7].

The use of the coolable sample stage allows IBIC imaging as a function of temperature, allowing the role of individual charge traps to be investigated. Fig. 2 shows an example of an IBIC image of the CCE distribution across a corner of a 2 mm thick cadmium zinc telluride (CZT) detector acquired at 250 K [8]. The data demonstrates the excellent charge transport uniformity of this device, and also shows some additional features due to a surface scratch (two vertical lines) and mechanical probing marks (regular grid of small dots). A vertically-aligned region of higher CCE, reaching 80%, is observed on the right hand edge of the image at this temperature, which was not observed at 300 K, due to the partial filling of electrical traps by charge produced from the ion beam.

Digital IBIC is a new extension of the regular IBIC technique that has been recently pioneered at the Surrey microbeam [9]. In this method, the analogue pulse processing amplifier, ADC and multichannel analyser is replaced by a high-speed waveform digitiser. This allows complete digital pulse shape analysis of the IBIC pre-amplifier output signal, giving measurements of charge drift velocity and mobility in bulk semiconductors.

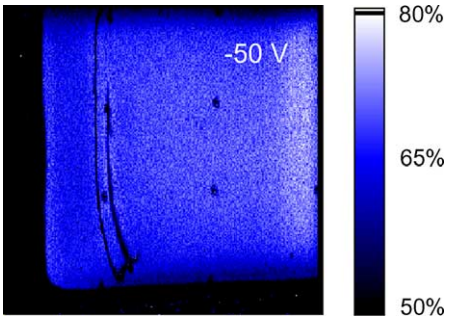


Fig. 2. IBIC image acquired at 250 K imaging the charge collection efficiency (between 50% and 80%) distribution across a corner of a 2 mm thick CZT detector; 50 V bias.

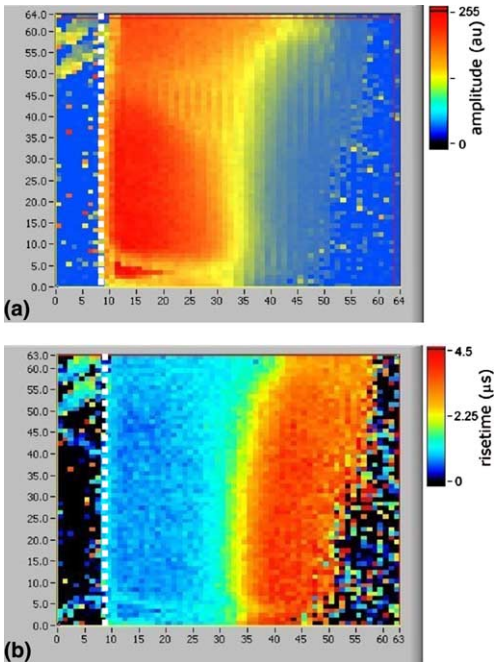


Fig. 3. Digital IBIC images acquired laterally through the side of a CZT detector, showing (a) pulse amplitude and (b) pulse risetime. The device cathode is indicated towards the left of the image, the anode is beyond the right edge.

Fig. 3 shows the first data acquired with the digital IBIC system where a 2.5 MeV He beam was used to laterally scan between the cathode and the anode of a CZT detector. Close to the cathode the induced signal is predominantly due to electron transport, and has a high amplitude. Conversely, close to the anode the induced signal is due to hole transport which produces a very small signal amplitude due to significant hole trapping (Fig. 3(a)). Regions of different amplitude response due to material non-uniformities are also clearly shown in Fig. 3(a). Fig. 3(b) shows the corresponding increase in signal risetime due to the increasing influence of the slow hole component of the total signal. Analysis of this data gives a room temperature electron drift mobility value of $1.1 \times 10^3$ cm$^2$/V s.

## 3. Millibeam line

The purpose of this beamline is to facilitate unattended automatic data collection on large

batches of samples, including routine RBS/ERD depth profiling and multiaxis channelling on single crystals. Depth profiles can be extracted automatically from the collected spectra using our DataFurnace [10] software. The millibeam line features a new 6 movement goniometer which has been designed and built by Arun Microelectronics Ltd. and which has a similar construction to that reported by Holländer et al. [11]. Samples can be loaded rapidly through an airlock. The whole mechanism is behind the sample stage so that glancing beam incident and beam exit geometries can be used.

Two backscattering particle detectors are installed at different scattering angles to help resolve ambiguities and to provide two independent data channels for data validation. A further particle detector with a range foil is mounted in a forward recoil direction for H profiling by ERD with a $^4$He beam. Other instrumentation includes a chopper with backscattered particle detector for independent beam current monitoring, and an alignment laser mounted behind the high energy magnet giving a beam coincident with the ion beam. A fixed video camera allows the samples to be viewed directly. Electrostatic deflection after the high energy magnet allows the beam to be switched off.

The goniometer has a vertical rotation axis with 363° of motion and 0.001° per step: stacked on top of this motion is a horizontal tilt axis perpendicular to the beam with 30° of motion and 0.0005° per step, and a rotation axis perpendicular to the tilt axis and normal to the sample stage surface with 210° of motion and 0.00025° per step. The axial motions have a maximum speed of 2000 steps/s. Linear $X$, $Y$, $Z$ motions are stacked on top of the axial motions, have a resolution of 0.004 mm per step and a maximum speed of 1500 steps/s.

The sample stage (Fig. 4) is $105\times153$ mm and slides into the mechanism, with push-fit electrical connections being made to allow current integration from the sample or other instrumentation. It has a 25 mm hole which can be aligned with a corresponding hole in the goniometer mechanism so that the beam can be passed through the instrument to the back of the chamber allowing a Faraday cup beam stop to be installed. Every part of the sample stage can be brought under the beam. A $Z$ motion of 5.6 mm perpendicular to the sample stage is used to make the plane of the sample surface intersect the eucentric point.

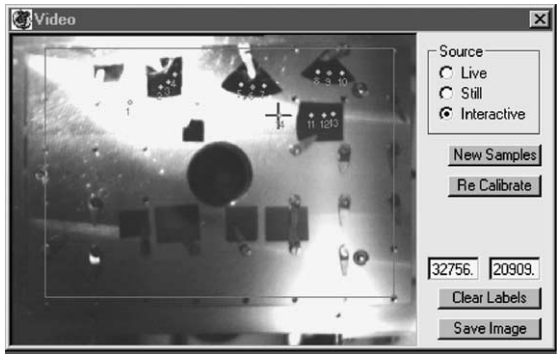


Fig. 4. The "DualTrace" program, video utility. The cross over 'Position 14' marks the current beam position. The absolute $X$, $Y$ position in steps is given in the two text windows. There are three numbered Positions on each of four samples. The rectangle framing the samples gives the calibration in mm of the video image. The hole in the centre of the sample plate allows beam transmission through the instrument.

"DualTrace" is a multipurpose data collection program written in VisualBasic which controls the goniometer, the video camera, three ADC cards in the PC, digital inputs from the current integrator and chopper, and digital outputs for the chamber light, the alignment laser and the beam switch. There are tools for setting the goniometer hardware limits of motion, and also the sample exchange and beam-normal positions. Other tools set various parameters of the ADCs, display the current spectra, display the video image and display the dual trace (of beam current and count rate) for channelling. We have also implemented a scripting language including branching structures which allow unattended data collection.

Fig. 4 shows the stored video image of a sample plate taken when the sample plate is square to the camera and with a pre-set $X$, $Y$, $Z$ position. This image has a standard calibration of the $X$, $Y$ position so that the beam position on the plate can be displayed continuously for any orientation of the plate, provided that the beam intersects the eucentric point and the latter is intersected by the sample surface. Because of the standard calibration, the stored image can be used to move any

part of the plate under the beam by "point and click". A series of pre-set Positions can be specified with "point and click" which can be used in the scripting language.

## Acknowledgements

The Ion Beam Centre and PKS acknowledge the financial support of EPSRC under grants GR/M94434/01, GR/R50097/01 and GR/R34486/01. We are very grateful for the contribution of Mark Browton in the beam line installation and Adrian Cansell for the machine operation.

## References

[1] D.J.W. Mous, A. Gottdanga, R. Van den Broek, R.G. Haitsma, Nucl. Instr. and Meth. B 99 (1995) 697.
[2] D.J.W. Mous, R.G. Haitsma, T. Butz, R.-H. Flagmeyer, D. Lehmann, J. Vogt, Nucl. Instr. and Meth. B 130 (1997) 31.
[3] G.W. Grime, M. Dawson, M. Marsh, I.C. McArthur, F. Watt, Nucl. Instr. and Meth. B 54 (1991) 52.
[4] M.B.H. Breese, D.N. Jamieson, P.J.C. King, Materials Analysis Using a Nuclear Microprobe, Wiley, New York, 1996.
[5] R. Szymanski, D.N. Jamieson, Nucl. Instr. and Meth. B 130 (1997) 80.
[6] G.W. Grime, Nucl. Instr. and Meth. B 109–110 (1996) 170.
[7] A. Simon, P. Sellin, A. Lohstroh, Nucl. Instr. and Meth. B, these Proceedings. doi:10.1016/j.nimb.2004.01.207.
[8] A. Lohstroh, P.J. Sellin, A. Simon, J. Phys.: Condens. Matter 16 (2004) 567.
[9] P.J. Sellin, A. Lohstroh, A. Simon, M.B.H. Breese, Nucl. Instr. and Meth. A 521 (2004) 600.
[10] C. Jeynes, N.P. Barradas, P.K. Marriott, G. Boudreault, M. Jenkin, E. Wendler, R.P. Webb, J. Phys. D 36 (2003) R97.
[11] B. Holländer, H. Heer, M. Wagener, H. Halling, S. Mantl, Nucl. Instr. and Meth. B 161 (2000) 227.